

**DETC2005-85315**

## **Planar Motion Generation Incorporating a 6-Link Mechanism and Non-Circular Elements**

Javier Roldán Mckinley  
Center for Intelligent Machines and Robotics  
University of Florida FL, USA  
jmckinrold@hotmail.com

David B. Dooner  
University of Puerto Rico at Mayagüez  
Mayagüez, Puerto Rico  
d\_dooner@me.uprm.edu

Carl Crane III  
Center for Intelligent Machines and Robotics  
University of Florida FL, USA  
ccrane@ufl.edu

Jean-Francois Kammath  
Center for Intelligent Machines and Robotics  
University of Florida FL, USA  
jfkamath@msn.com

### **ABSTRACT**

This work is a specific application of a particular one degree of freedom six-link geared planar mechanism. A procedure to synthesize non-circular gear pitch profiles to generate any prescribed function of position and orientation in a determined range is presented. The geometry of the mechanism, i.e. the link lengths of the six-bar mechanisms, is assumed known. The input parameters are the prescribed path, the orientation angle at each position along the path, and the interval along which the motion is required. A generic function  $y=f(x)=ax^2+bx+c$ , in a particular interval of  $x$ , was used to define the desired path. The desired orientation of the coupler link was specified as being tangent to the path at each point. An analysis was performed and complete non-circular profiles were successfully synthesized. Numerical examples are presented.

### **INTRODUCTION**

The use of non-circular gear elements to perform a desired relationship has been in existence for many years. In the middle of 18<sup>th</sup> century, Holditch[1] treated the rolling of non-circular curves. Cunningham[2] also proposed later the generation of mathematical functions using non-circular gears in the middle of the 20<sup>th</sup> century.

In spite of the antiquity of non-circular gears, few studies have been done to get the integration of motion generation by non-circular gears into planar and spatial mechanisms. The majority of studies are related to function generation. Early works about geared mechanisms were focused on geared five-bar linkages. Freudenstein and Primrose[3] derived algebraic, geometric, and kinematical properties for the curve generated by a point on the axis of the joint connecting the two floating links of a geared five-bar mechanism for an arbitrary

commensurate gear ratio. Roth and Freudenstein[4] proposed the synthesis of path generation for the geared five-bar mechanism by numerical methods applied to nine precision points. Oleksa and Tesar[5] also employed the geared five-bar to achieve a function generator's design for five different positions. Separately, Erdman and Sandor[6] showed the kinematical synthesis of a geared five-bar function generator, a general closed form method of planar kinematical synthesis using complex numbers to represent the vector loop equation.

In reference to six-link mechanisms, the Stephenson's six bar inversions I, II and III mechanisms, and Watt's six-bar inversions I and II mechanisms have been synthesized in depth (e.g. see McLarnan [7]), but these are not geared linkages. On the other hand, Rao and Sandor[8] developed an extension of Freudenstein's equation to geared linkages to achieve a geared (circular gears) six-bar linkage function generator for five and six point approximation.

Similar works to this research are now presented. Dimaragonas, Erdman and Sandor[9] utilized complex number and matrix methods to develop a general geared n-bar function generator. They also included circular gears in the transmissions and proposed a systematic way of finding the gear ratio for each circular gear pair of the circular geared n-bar linkage proposed. Rao, Sandor and Kramer[10] utilized complex number methods to synthesize and analyze the six-bar geared path generation for five, six, and seven prescribed path points with prescribed path rotations; the linkage only used one gear transmission and one gear was fixed to ground. More recently, Dooner[11] summarized a function generator using an eight-link mechanism with optimized non-circular gear elements where he included the coordinated steering of automobiles as an illustrative application.

Diverse applications of the non-circular gears have also been developed. For instance, Han[12] proposed the use of non-circular gears for balancing of the shaking moment in spatial linkages. Emura and Arakawa[13] included a new steering mechanism using non-circular gears. Dooner[14] suggested non-circular gears to reduce torque and speed fluctuations in rotating shafts. Similarly, Yao and Yan[15] also used non-circular gears for torque balancing of planar linkage. Likewise, Kochev[16] proposed non-circular gears to provide necessary rotation to eliminate completely the shaking moment in planar linkages. Manufacturing aspects about non-circular gears have also been treated lately (see Figliolini and Angeles[17]). More literature about the kinematical considerations of non-circular gears has been written by Litvin[18], Dooner and Seireg[19], and Dooner[20].

In this paper, a general and novel method of solving the path and orientation problem for the planar case is presented. The kinematical synthesis involved is classified as a dimensional synthesis to satisfy motion generation via an analytical method. The approach presented below utilizes a six-link mechanism with mobility equal to one, and two non-circular gears pairs to achieve generalized motion generation with respect to an inertial reference frame. Figure 1 displays the six-link 6R<sup>1</sup> mechanism with non-circular gears proposed. Motion is defined by a given Cartesian path  $(x, f(x))$  and an orientation angle  $\sigma$ . The link lengths, the ground angle, and the coupler angle are known parameters. First, the inverse kinematic problem is solved. Next, the input/output (I/O) non-circular gear pitch profiles are determined. The solution involves highly non-linear equations for the mechanism variables. The I/O non-circular gear relationships are non-linear equations also. Finally, a known mathematical function is generated along a specific interval for a specified orientation angle of the coupler. Only partial non-circular pitch profiles are needed to achieve the desired motion; however, the profile can be usually synthesized for a complete rotation.

The scope of the current work is limited to the gear profile synthesis problem. This implies that no manufacturing details, no tooth profile analysis, no rating (stress, noise and vibrations, fatigue, etc.), and no backlash issues are considered. It is also implied that paths with one value of ordinate per each value of the abscissa can only be successfully developed via this technique.

**NOMENCLATURE**

- $a, b, c$  = Constants of the quadratic function
- $c_i$  = Coefficients of fourth-degree polynomial
- $E$  = Center distance
- $f(x)$  = Function of the variable  $x$
- $g_i$  = I/O relationship of the  $i$ -th transmission
- $g'_i$  = First derivative of  $g_i$

- $I/O$  = Input/Output gear relationship
- $J_1, J_2$  = Number of full and half joints
- $l_1, \dots, l_6$  = Link lengths 1 to 6
- $M$  = Mobility or Degrees of Freedom
- $N$  = Number of links
- $P$  = Point attached to body 4
- $\rho_4, \rho_4$  = Lengths associated to body 4
- $x$  = Independent variable
- $x_0, x_f, \Delta x$  = Lower limit, upper limit, increment of  $x$
- $\gamma_1, \gamma_2$  = Angles associated with body 4
- $\eta(x)$  = Angle between path tangency and  $x$  axis
- $\theta_{int}$  = Input angle final value at working section
- $\theta_1, \dots, \theta_6$  = Link angles 1 to 6
- $\theta'_2, \dots, \theta'_6$  = First derivative of  $\theta_2, \dots, \theta_6$  respect to  $x$
- $\theta''_2, \dots, \theta''_6$  = Second derivative of  $\theta_2, \dots, \theta_6$  respect to  $x$
- $\sigma$  = Orientation angle

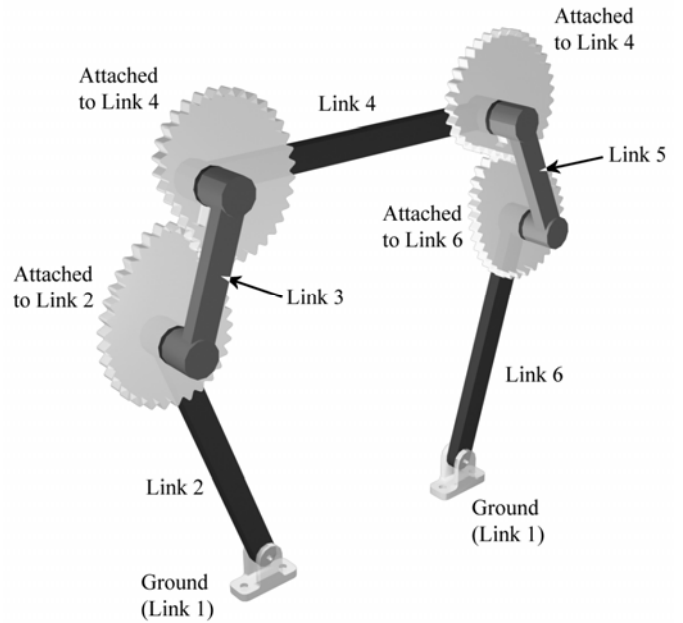


**Fig. 1 6-link 6R mechanism with non-circular gears**

**1 BACKGROUND**

There are applications in industry where it is necessary that a body traverses a particular path and orientation with respect to a certain reference frame. Some applications include automotive suspension systems, garbage truck delivery, shoe testing machine, and painting process. The synthesis of a mechanism to achieve such a task is known as motion generation.

Before developing the motion generation method proposed in this report, a brief mobility analysis is presented to emphasize

<sup>1</sup> R: Standard notation for revolute joint

the effect of the two gear connections in the 6-link 6R planar mechanism. Select gearing topics relevant to this report are also included in this section.

### 1.1 SIX-BAR MECHANISM

Figure 2 shows a planar 6-link 6R mechanism. This linkage is an unconstrained kinematic chain because its mobility is higher than 1. The modified Gruebler's equation to determine the mobility of a planar mechanism is

$$M = 3(N - 1) - 2J_1 - J_2 \tag{1}$$

where:

$M$ : mobility or Degrees of Freedom (DOF)

$J_1$ : number of full joints

$J_2$ : number of roll-slide contact joints

$N$ : number of links.

The six-bar linkage depicted in Fig. 1 possesses mobility 3. Two gear connections are added to the mechanism as shown in Fig. 1. Thus  $J_2$  now equals 2 for this case and the combination of an unconstrained six-link kinematic chain and two gear connections results in a one degree of freedom device.

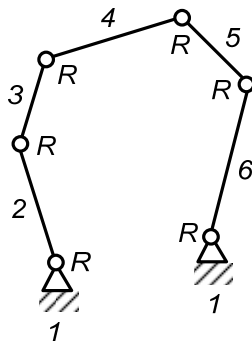


Fig. 2 Six-link unconstrained kinematic chain

### 1.2 GEARING CONSIDERATIONS

The angular displacements of two toothed bodies in perfect mesh (no slipping) define a ratio that characterizes the motion. This is the Input/Output (I/O) non-circular gear relationship. Input and output angles are defined as the angular displacements of the input and output bodies in mesh, respectively. How to relate the angular displacements and the I/O non-circular gear relationship are explained in this section. Finally, equations to graphically present the pitch profiles are included.

#### 1.2.1 Input/Output Non-Circular Gear Relationship

The transmission function for two bodies in mesh is defined as the relationship between the angular position of the input

element and the corresponding angular position of the output element. Dooner [22] stated a first law of gearing as follows: "For any given axes, the contact normal must be reciprocal to the instantaneous twist in order to achieve the desired instantaneous gear ratio." This statement for the first law of gearing is valid for circular and non-circular gears in mesh. Accordingly, it can be written as

$$g \equiv \frac{d\theta_o}{d\theta_i} \tag{2}$$

where:

$g$ : instantaneous gear ratio or I/O relationship

$d\theta_o$ : instantaneous angular displacement of the output body

$d\theta_i$ : instantaneous angular displacement of the input body.

Figure 3 depicts the geared transmissions with the links  $j-1$ ,  $j$ , and  $j+1$  all movable. The recurrent equation for the I/O non-circular relationship is given by Eq. (3). The angles  $\theta_{j-1}$ ,  $\theta_j$ , and  $\theta_{j+1}$  are the net angular displacements. These are measured respect to the fixed  $x$  axis.

$$g_j = \frac{d(\theta_{j+1} - \theta_j)}{d(\theta_j - \theta_{j-1})} \tag{3}$$

where:

$g_j$ : I/O relationship of the transmission

$d\theta_j$ : instantaneous angular displacement of the  $j$ -th link.

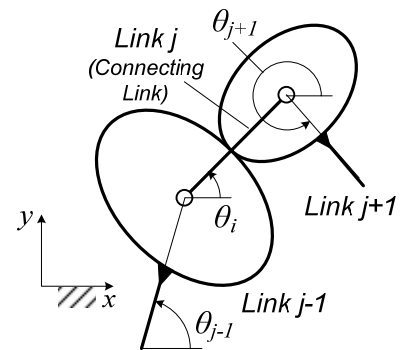
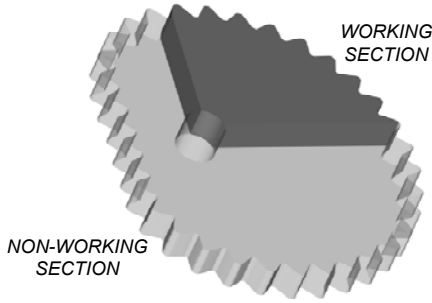


Fig. 3 Non-circular gears all links moving

#### 1.2.2 Synthesis of the Complete Profile: Non-Circular Relationships for the Whole Rotation

Some real applications of toothed bodies are fulfilled by partial circular or non-circular gears, where the covered angle is less than  $2\pi$ . An example is the Bourdon manometer. However, a complete profile is sometimes required for manufacturing purposes. To this end, working and non-working sections of the profile are now introduced. The working profile refers to the section of the gear that is really needed to perform a task. The non-working profile is the remaining section that converts the working slice into a

complete disk. Figure 4 shows a complete non-circular gear with arbitrary working and non-working sections.



**Fig. 4 Working and non-working sections**

If the working section is circular, it is evident that the complete profile becomes a conventional circular gear. If non-circularity is the case, some geometric considerations must be taken into account to achieve a complete non-circular gear profile.

The I/O non-circular relationship corresponding to the working section is written as  $g_w$ . Similarly, the I/O relationship for the non-working section is labeled by  $g_{nw}$ . The geometric considerations to obtain the non-working section are discussed below.

When the I/O relationship is not specified for the complete rotation, the  $2\pi$ -relationship can be achieved by introducing a fourth-degree polynomial at the  $g$  domain

$$g_{nw}(\theta_i) = c_4\theta_i^4 + c_3\theta_i^3 + c_2\theta_i^2 + c_1\theta_i + c_0 \quad (4)$$

where:

$\theta_i$ : input angle

$g_{nw}$ : non-working I/O gear relationship

$c_i$ : fourth-degree polynomial's coefficients.

The fourth-degree polynomial's coefficients of Eq. (4),  $c_i$ , are found via five boundary conditions. Figure 5 illustrates four constraints required to guarantee a continuous profile, where  $\theta_{int}$  makes reference to the final value of the input angle for the working section.

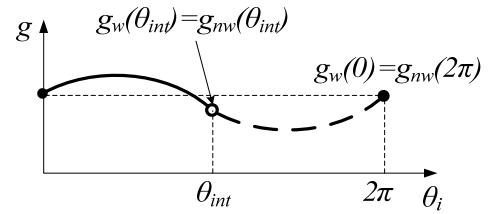
The I/O non-circular gear relationship must satisfy another particular constraint to successfully synthesize a complete profile. The integral shown in Eq. (5) must be always rational, otherwise, the output gear could not maintain an indefinite number of cycles with the desired functional relationship (Dooner and Seireg [19]):

$$2\pi = \int_0^{2\pi} g d\theta_i \quad (5)$$

where:

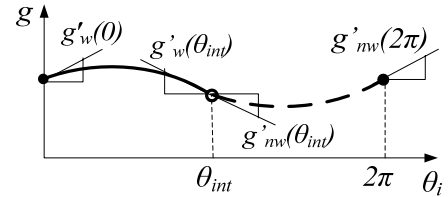
$g$ : instantaneous gear ratio or I/O relationship

$d\theta_i$ : instantaneous angular displacement of the input body.



(a)  $g$  boundary conditions

$$g'_w(0) = g'_{nw}(2\pi) \quad g'_w(\theta_{int}) = g'_{nw}(\theta_{int})$$



(b)  $g'$  (slope) boundary conditions

———— Working profile section  
 - - - - Non-working profile section

**Fig. 5 Boundary conditions for whole continuous profile synthesis**

From Fig. 5 and the constraint imposed by Eq. (5), the five boundary conditions are

$$g_w(\theta_{int}) = g_{nw}(\theta_{int}) \quad (6)$$

$$g'_w(\theta_{int}) = g'_{nw}(\theta_{int}) \quad (7)$$

$$g_w(0) = g_{nw}(2\pi) \quad (8)$$

$$g'_w(0) = g'_{nw}(2\pi) \quad (9)$$

$$\int_{\theta_0=0}^{\theta_{int}} g_w d\theta_i + \int_{\theta_{int}}^{2\pi} g_{nw} d\theta_i = 2\pi \cdot \quad (10)$$

It is apparent that Eq. (10) is derived from Eq. (5) and the linearity principle for the integral.

Equations (6) to (10) are a set of linear equations representing the unknown coefficients  $c_1, \dots, c_5$  of Eq. (4). The solution for the coefficients can be written in the matrix format

$$C = \Omega^{-1}H \quad (11)$$

where:

$$C = \begin{bmatrix} c_4 \\ c_3 \\ c_2 \\ c_1 \\ c_0 \end{bmatrix}, \quad H = \begin{bmatrix} g_w(\theta_1) \\ g'_w(\theta_1) \\ 2\pi \\ g'_w(0) \\ 2\pi - \int_0^{\theta_1} g_w(\theta_i) d\theta_i \end{bmatrix}$$

specific to the 6-link, 6-R mechanism is solved in the next section.

$$\Omega = \begin{bmatrix} \theta_{\text{int}}^4 & \theta_{\text{int}}^3 & \theta_{\text{int}}^2 & \theta_{\text{int}} & 1 \\ 4\theta_{\text{int}}^3 & 3\theta_{\text{int}}^2 & 2\theta_{\text{int}} & 1 & 0 \\ (2\pi)^4 & (2\pi)^3 & (2\pi)^2 & (2\pi) & 1 \\ 4(2\pi)^3 & 3(2\pi)^2 & 2(2\pi) & 1 & 0 \\ \frac{(2\pi)^5 - \theta_{\text{int}}^5}{5} & \frac{(2\pi)^4 - \theta_{\text{int}}^4}{4} & \frac{(2\pi)^3 - \theta_{\text{int}}^3}{3} & \frac{(2\pi)^2 - \theta_{\text{int}}^2}{2} & 2\pi - \theta_{\text{int}} \end{bmatrix}.$$

At this point,  $g$  has been completely derived for the non-working profile. In addition, the input and output angles need to be specified for the complete profile synthesis.

It is apparent from Fig. 5 that the input angle for the non-working section is given by

$$\theta_{\text{inv}} = 2\pi - \theta_{\text{int}}. \quad (12)$$

The expression for the output angle at the non-working section is obtained by solving for the output angle in Eq. (2), where the expression for  $g$  is given by Eq. (4). The compact format equation is

$$\theta_{\text{out}} = \sum_{i=0}^4 \frac{c_i}{i+1} \left[ (2\pi)^{i+1} - (\theta_{\text{int}})^{i+1} \right] \quad (13)$$

where:

$c_i$ : coefficients in polynomial of Eq. (4).

### 1.2.3 Pitch Curve

Equations that relate the input angles, output angles, and the I/O relationships in order to obtain the pitch curve coordinates are presented here. Figure 6 introduces the center distance,  $E$ , as an additional parameter. This plot also defines two rectangular coordinate systems used to describe the pitch curves of the input and the output bodies.

The input and output radii are related by

$$r_o + r_i = E. \quad (14)$$

The I/O relationship is introduced to add one more equation. For the two bodies in mesh shown in Fig. 6,  $g$  becomes

$$g = \frac{r_i}{r_o}. \quad (15)$$

Equations (14) and (15) form a system of two equations in the two unknowns  $r_o$  and  $r_i$ . The radii expressions are

$$r_o = \frac{E}{1+g} \quad (16)$$

$$r_i = E \frac{g}{1+g}. \quad (17)$$

The required gearing considerations for the synthesis of the non-circular profiles have been presented. Motion generation

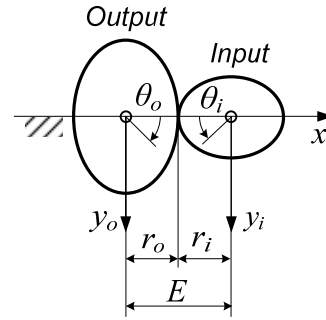


Fig. 6 Rectangular coordinate systems  $x-y_o$  and  $x-y_i$  for a gear pair in mesh

## 2 PLANAR MOTION GENERATION WITH A SIX-LINK MECHANISM AND NON-CIRCULAR GEARS

The solution of the motion generation problem starts with the inverse kinematic stage. Mechanism parameters (ground angle, link lengths, and coupler angles) have been previously specified. The position angles are to be determined based on the mechanism parameters and required path and orientation of the coupler link.

The working range input and output angles in addition to the I/O non-circular relationships are firstly obtained based on a position analysis. It follows the attainment of non-working angles and I/O relationship expressions.

### 2.1 INVERSE KINEMATICS

The mechanism parameters are known values that completely define the geometry of the mechanism. These parameters are the link lengths and the position of the control point on the coupler link. Figure 7 shows the mechanism parameters. The link lengths are  $l_1, l_2, l_3, l_4, l_5$  and  $l_6$ . The follower (body 4) is defined by its link length  $l_4$ , the distances  $\rho_4$  and  $p_4$ , and the angles  $\gamma_1$  and  $\gamma_2$ . The ground angle  $\theta_1$  is also a mechanism parameter.

The orientation of each link is specified by the link angles  $\theta_2, \theta_3, \theta_4, \theta_5$ , and  $\theta_6$  where the orientation of body 4 is specified by the angle  $\theta_4$ . These angles are taken in the counterclockwise sense and measured at the indicated positions as depicted in Fig. 7.

Figure 7 also displays the motion generation requirements defined by a path and an orientation for body 4. The path is given by the coordinates  $(x, f(x))$  to be followed by point  $\mathbf{P}$  in body 4. Orientation is specified by  $\sigma$ , which is defined as the angle between the normal to link 4 and the path tangency, as depicted in Fig. 7.

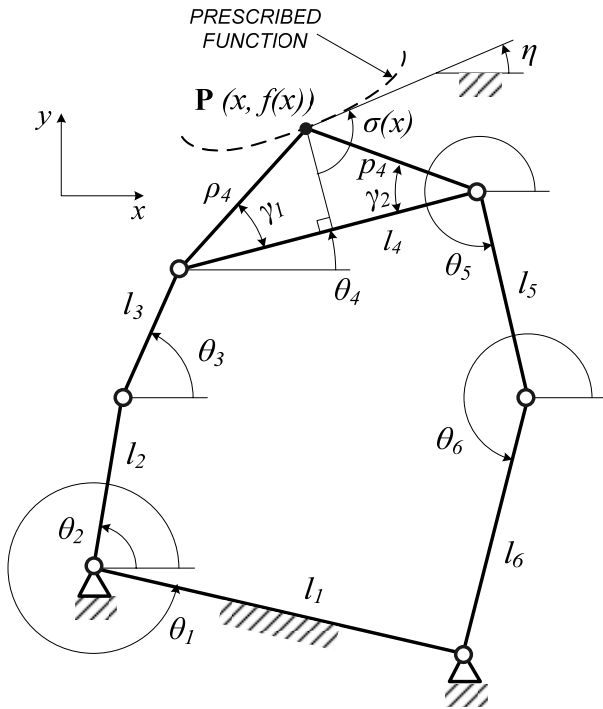


**Fig. 7 Six-link mechanism parameters and motion generation requirements**

One additional parameter,  $\eta$ , is introduced to control the orientation angle of the coupler.  $\eta$  defines the angle between the path tangency and the horizontal axis according to the Cartesian system established. The relationship among these angles is given by

$$\eta(x) = \arctan(f'(x)) \quad (18)$$

$$\sigma(x) = \eta(x) - \theta_4 + \frac{\pi}{2} \quad (19)$$

where:

$\sigma(x)$ : angle between the path tangency and the perpendicular to link 4

$\eta(x)$ : angle between path tangency and horizontal axis

$\theta_4$ : link 4 angle.

Position and orientation can only be achieved along a certain interval  $[x_o, x_f]$ , where  $x_o$  and  $x_f$  are the lower and upper boundary of the interval to be swept.

The inverse kinematic problem will now be solved. The governing equations necessary to determine  $\theta_2, \theta_3, \theta_4, \theta_5$  and  $\theta_6$  in the six-link mechanism are to be found. Figure 8 shows the vector loop closure for the six-link mechanism.

From Fig. 8, the vector loop equation for the x-component passing through links 2-3-4 gives

$$l_2 \cos \theta_2 + l_3 \cos \theta_3 + \rho_4 \cos(\gamma_1 + \theta_4) = x. \quad (20)$$

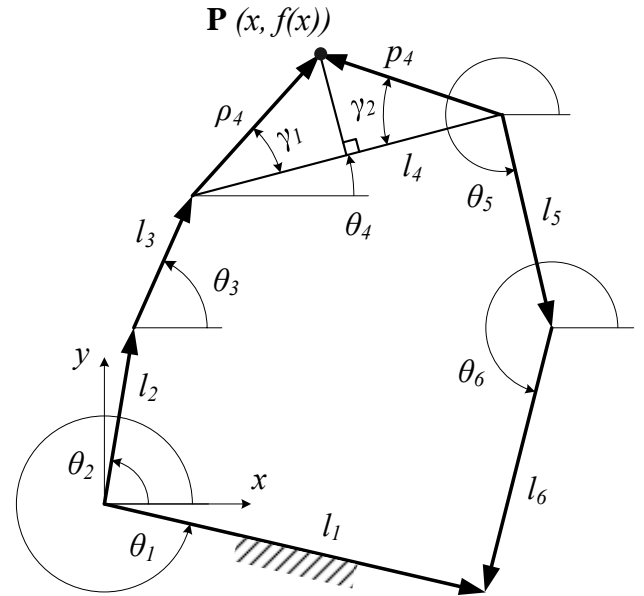


**Fig. 8 Vector loop for the six-link mechanism**

For the y-component along the links 2-3-4, it is obtained

$$l_2 \sin \theta_2 + l_3 \sin \theta_3 + \rho_4 \sin(\gamma_1 + \theta_4) = f(x). \quad (21)$$

Similarly, the x-component for links 1-5-6-4 gives

$$-l_1 \cos \theta_1 + l_5 \cos \theta_5 + l_6 \cos \theta_6 - p_4 \cos(\pi - \gamma_2 + \theta_4) = -x \quad (22)$$

For the y-component along the links 1-5-6-4, it is now obtained that

$$-l_1 \sin \theta_1 + l_5 \sin \theta_5 + l_6 \sin \theta_6 - p_4 \sin(\pi - \gamma_2 + \theta_4) = -f(x) \quad (23)$$

One more equation is needed to obtain a determined system of equations. This equation is obtained from Eq. (18) as

$$\theta_4 = \frac{\pi}{2} + \arctan \frac{df(x)}{dx} - \sigma. \quad (24)$$

The set of equations (19) to (24) can be solved as follows. The angle  $\theta_4$  depends on the derivative of the prescribed function and angle between the path tangency and the perpendicular to the coupler, already specified. Therefore, the system is reduced to four equations, i.e. Eqs. (20) to (24), in the four unknowns:  $\theta_2, \theta_3, \theta_5$  and  $\theta_6$ . The solution is presented in Eqs. (25) to (28) as

$$\theta_2(x) = 2 \arctan \left[ \frac{-\beta_2 \pm \sqrt{\beta_2^2 - 4\alpha_2\phi_2}}{2\alpha_2} \right] \quad (25)$$

where:

$$\beta_2 = -2[f(x) - \rho_4 \sin(\gamma_1 + \theta_4)]$$

$$\alpha_2 = \frac{(x - \rho_4 \cos(\gamma_1 + \theta_4))^2 + \left(\frac{\beta_2}{2}\right)^2 + l_2^2 - l_3^2}{2l_2} + x - \rho_4 \cos(\gamma_1 + \theta_4)$$

$$\phi_2 = \frac{(x - \rho_4 \cos(\gamma_1 + \theta_4))^2 + \left(\frac{\beta_2}{2}\right)^2 + l_2^2 - l_3^2}{2l_2} - x + \rho_4 \cos(\gamma_1 + \theta_4)$$

$$\theta_3(x) = 2 \arctan \left[ \frac{-\beta_2 \pm \sqrt{\beta_2^2 - 4\alpha_3\phi_3}}{2\alpha_3} \right] \quad (26)$$

where:

$$\alpha_3 = \frac{(x - \rho_4 \cos(\gamma_1 + \theta_4))^2 + \left(\frac{\beta_2}{2}\right)^2 + l_3^2 - l_2^2}{2l_3} + x - \rho_4 \cos(\gamma_1 + \theta_4)$$

$$\phi_3 = \frac{(x - \rho_4 \cos(\gamma_1 + \theta_4))^2 + \left(\frac{\beta_2}{2}\right)^2 + l_3^2 - l_2^2}{2l_3} - x + \rho_4 \cos(\gamma_1 + \theta_4)$$

$$\theta_5(x) = 2 \arctan \left[ \frac{-\beta_5 \pm \sqrt{\beta_5^2 - 4\alpha_5\phi_5}}{2\alpha_5} \right] \quad (27)$$

where:

$$\beta_5 = 4\Sigma l_5$$

$$\alpha_5 = -(\Sigma^2 + \Psi^2 + l_5^2 - l_6^2) - 2\Sigma l_5$$

$$\phi_5 = 2\Sigma l_5 - (\Sigma^2 + \Psi^2 + l_5^2 - l_6^2)$$

where:

$$\Sigma = x - p_4 \cos(\pi - \gamma_2 + \theta_4) - l_1 \cos \theta_1$$

$$\Psi = f(x) - p_4 \sin(\pi - \gamma_2 + \theta_4) - l_1 \sin \theta_1$$

$$\theta_6(x) = 2 \arctan \left[ \frac{-\beta_5 \pm \sqrt{\beta_5^2 - 4\alpha_6\phi_6}}{2\alpha_6} \right] \quad (28)$$

where:

$$\alpha_6 = -(\Sigma^2 + \Psi^2 + l_6^2 - l_5^2) - 2\Sigma l_6$$

$$\phi_6 = 2\Sigma l_6 - (\Sigma^2 + \Psi^2 + l_6^2 - l_5^2)$$

where  $\Sigma$  and  $\Psi$  were defined in Eq. (27).

Because of the quadratic solutions for  $\theta_2$ ,  $\theta_3$ ,  $\theta_5$ , and  $\theta_6$ , there are also two solutions for the non-circular pitch profile. The inverse kinematic problem is solved at this point. The next section considers the synthesis of the profiles based on the results obtained here.

## 2.2 NON-CIRCULAR PROFILE SYNTHESIS

Once the inverse kinematics problem is solved, the next task is finding the input and output angles in addition to the I/O relationships for working and non-working sections. To this

end, a notation is first presented according to that offered in Eq. (3) and Fig. 3.

I/O relationships will be labeled accordingly with the number of the connecting link. For example, gears that attach links 2-3-4 are defined as connection 234. Link 3 is the connecting element and  $g_3$  labels the I/O relationship for this connection. Analogously,  $g_5$  is the I/O relationship for the connection 456 where link 5 is the connecting element for links 4-5-6. Equations (29) and (30) are the I/O relationships obtained by direct application of Eq. (3) to connections 234 and 456, respectively.

$$g_3 = \frac{d(\theta_4 - \theta_3)}{d(\theta_3 - \theta_2)} \quad (29)$$

$$g_5 = \frac{d(\theta_6 - \theta_5)}{d(\theta_5 - \theta_4)} \quad (30)$$

These equations are also useful to define the input and output angles of connections 234 and 456. The input angles are obtained by comparing Eq. (2) with Eqs. (29) and (30) to obtain

$$\theta_{i3} = \theta_3(x) - \theta_2(x) \quad (31)$$

$$\theta_{i5} = \theta_6(x) - \theta_5(x) \quad (32)$$

Analogously, the output angles for connections 234 and 456 are

$$\theta_{o3} = \theta_4(x) - \theta_3(x) \quad (33)$$

$$\theta_{o5} = \theta_5(x) - \theta_4(x) \quad (34)$$

Expressions obtained in this section will support the working and non-working profile synthesis.

### 2.2.1 Working Profile

Equations (33) and (34) are the expressions for the working I/O relationships. The solutions to the instantaneous angular displacements involved can not be readily calculated. The unitary ratio  $dx/dx$  will be introduced into these equations to achieve expressions for the I/O relationships that are much easier to evaluate. These are

$$g_3 = \frac{\frac{d\theta_4}{dx} - \frac{d\theta_3}{dx}}{\frac{d\theta_3}{dx} - \frac{d\theta_2}{dx}} \quad (35)$$

$$g_5 = \frac{\frac{d\theta_6}{dx} - \frac{d\theta_5}{dx}}{\frac{d\theta_5}{dx} - \frac{d\theta_4}{dx}} \quad (36)$$

The required derivatives are now easy to obtain. Equation (37) is the derivative of  $\theta_4$  respect to  $x$ , found directly from Eq. (24). The remaining angle derivatives are obtained by Eq. (38), where the system of equations was established based on Eqs. (20) to (23). The I/O relationship is totally known at this point.

$$\frac{d\theta_4}{dx} = \frac{\frac{d^2 f(x)}{dx^2}}{1 + \left(\frac{df(x)}{dx}\right)^2} - \frac{d\sigma}{dx} \quad (37)$$

$$\Theta = \Delta^{-1} X \quad (38)$$

where:

$$\Theta = \begin{bmatrix} \theta_2' \\ \theta_3' \\ \theta_5' \\ \theta_6' \end{bmatrix}, \quad \Delta = \begin{bmatrix} l_2 \sin \theta_2 & l_3 \sin \theta_3 & 0 & 0 \\ l_2 \cos \theta_2 & l_3 \cos \theta_3 & 0 & 0 \\ 0 & 0 & l_5 \sin \theta_5 & l_6 \sin \theta_6 \\ 0 & 0 & l_5 \cos \theta_5 & l_6 \cos \theta_6 \end{bmatrix},$$

$$X = \begin{bmatrix} -1 - \rho_4 \sin(\gamma_1 + \theta_4) \theta_4' \\ f'(x) - \rho_4 \cos(\gamma_1 + \theta_4) \theta_4' \\ -1 - p_4 \sin(\pi - \gamma_2 + \theta_4) \theta_4' \\ f'(x) - p_4 \cos(\pi - \gamma_2 + \theta_4) \theta_4' \end{bmatrix}.$$

The input and output angles for the working profile are also required. They are obtained by substitution of Eqs. (24) to (28) into Eqs. (31) to (34).

## 2.2.2 Non-Working Profile

Non-working angles and I/O relationships for the non-working profile were described in Section 1.2.1, where five boundary conditions were established. Attention is addressed to Eqs. (7) and (9), in which the first derivative of the I/O relationship with respect to the input angle appears. It is then necessary to determine the derivative of the I/O relationships with respect to the input angle,  $\theta_i$ , for each connection, they are

$$g_3' = \frac{dg_3}{d\theta_{i3}} \quad (39)$$

$$g_5' = \frac{dg_5}{d\theta_{i5}} \quad (40)$$

More familiar expressions for  $g'$  arise from the substitution of Eqs. (29) and (31) into Eq. (39), and Eqs. (30) and (32) into Eq. (40) to obtain

$$g_3' = \frac{d\left(\frac{d(\theta_4 - \theta_3)}{d(\theta_3 - \theta_2)}\right)}{d(\theta_3 - \theta_2)} \quad (41)$$

$$g_5' = \frac{d\left(\frac{d(\theta_6 - \theta_5)}{d(\theta_5 - \theta_4)}\right)}{d(\theta_5 - \theta_4)} \quad (42)$$

The unitary ratio  $dx/dx$  is again introduced in Eqs. (41) and (42) to obtain

$$g_3' = \frac{(\theta_4'' - \theta_3'')(\theta_3' - \theta_2') - (\theta_4' - \theta_3')(\theta_3'' - \theta_2'')}{(\theta_3' - \theta_2')^3} \quad (43)$$

$$g_5' = \frac{(\theta_6'' - \theta_5'')(\theta_5' - \theta_4') - (\theta_6' - \theta_5')(\theta_5'' - \theta_4'')}{(\theta_5' - \theta_4')^3} \quad (44)$$

where:

$$\theta_2', \dots, \theta_6' = \frac{d\theta_2}{dx}, \dots, \frac{d\theta_6}{dx}; \quad \theta_2'', \dots, \theta_6'' = \frac{d^2\theta_2}{dx^2}, \dots, \frac{d^2\theta_6}{dx^2}.$$

Equation (45) is the second derivative of  $\theta_4$  respect to  $x$ , found directly from Eq. (37).

$$\theta_4'' = \frac{\left(1 + \left[\frac{df(x)}{dx}\right]^2\right) \frac{d^3 f(x)}{dx^3} - 2 \left[\frac{d^2 f(x)}{dx^2}\right]^2 \frac{df(x)}{dx}}{\left(1 + \left[\frac{df(x)}{dx}\right]^2\right)^2} - \frac{d^2 \sigma}{dx^2} \quad (45)$$

The second derivatives of  $\theta_2$ ,  $\theta_3$ ,  $\theta_4$ ,  $\theta_5$ , and  $\theta_6$  with respect to  $x$  can be readily obtained from Eq. (38). The resulting expression is too long and is not presented here.

Once  $g'$  is known, the five boundary conditions to obtain the fourth degree polynomial coefficients of Eq. (4) can be evaluated so that  $g$  is completely specified for the non-working profile. The input angle was previously defined in Eq. (12) and the output angle was found by Eq. (13). This ends the non-working section analysis.

One more step is missing to complete the synthesis of the pitch profiles; it applies for both working and non-working sections. Equations (16) and (17) can be used to obtain the input and output radii. The missing parameter is the center distance  $E$ . By comparison of Figs. 6 and 7,  $l_3$  and  $l_5$  are the center distances for the connections 234 and 456, respectively. It is now possible to obtain a plot of the entire pitch profile.

Here ends the profile synthesis process. It included an inverse kinematics stage followed by the synthesis of the working and non-working profile sections.

Figure 9 shows a flowchart that provides a brief summary of the overall process. The illustrative example presented in the following section was performed using a computer program based on steps presented in Fig. 9.



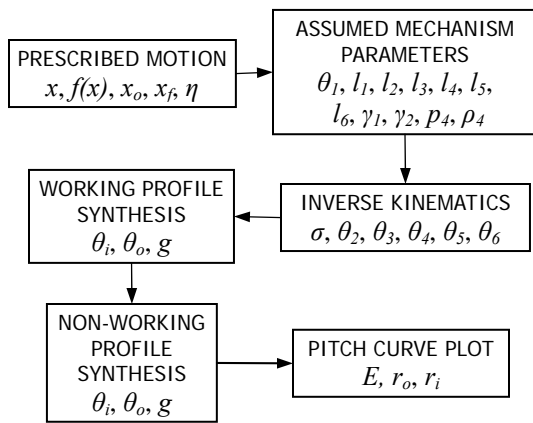


Fig. 9 Profile synthesis stages

### 3 RESULTS AND COMMENTS. MOTION GENERATION FOR $f(x) = ax^2+bx+c$

As a practical illustration of the method, the quadratic function is prescribed along a specific interval with a constant orientation angle relative to the tangent to the path. Working and non-working gear relationships are obtained. The complete profiles with the mechanism are also depicted.

The quadratic function is selected to be “motion-generated” along the interval  $20mm \leq x \leq 80mm$ . The orientation angle,  $\sigma$ , is constant, stated as  $\sigma = 80^\circ$ . Table 1 shows the values of the coefficients  $a$ ,  $b$ , and  $c$ , the mechanism parameters, and the motion requirements. A new parameter  $\Delta x$  is introduced, which is the spacing between the  $x$ -coordinates of the successive positions of point P in body 4.

Table 1 Input parameters in motion generation of  $f(x) = ax^2+bx+c$

Param.	Value	Param.	Value
$a$ [1/mm]	-2.3696E-3 (-9.3268E-5in <sup>-1</sup> )	$l_2$ [mm]	200 (7.8740in)
$b$ [-]	0.2367	$l_3$ [mm]	160 (6.2992in)
$c$ [mm]	418.325 (16.4695in)	$l_4$ [mm]	200 (7.8740in)
$\sigma$ [deg]	80	$l_5$ [mm]	220 (8.6614in)
$\theta_1$ [deg]	43.8	$l_6$ [mm]	180 (7.0866in)
$\gamma_1$ [deg]	49	$x_o$ [mm]	20 (0.7874in)
$\rho_4$ [mm]	145 (5.7087in)	$x_r$ [mm]	80 (3.1496in)
$l_1$ [mm]	500 (19.6850in)	$\Delta x$ [mm]	0.5 (1.9685E-2in)

Two geometrical solutions for the six-link mechanism are presented in Fig. 10. The increment,  $\Delta x$  was increased to 10mm (0.394in) in these plots to facilitate the understanding. The two configurations depicted in Fig. 10 correspond to the quadratic solution presented in Eqs. (25) to (28) for the position problem.

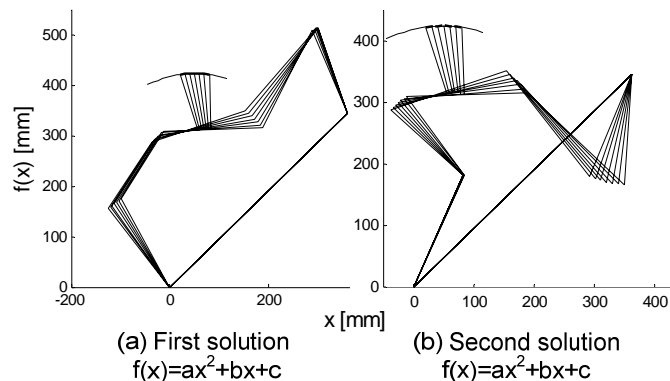


Fig. 10 Motion generation of  $f(x) = ax^2+bx+c$   
(a) 1st solution (b) 2nd solution

From here, the results presented correspond to the second solution configuration depicted in Fig. 10(b). Figure 11 displays the link angles reached for every link at every  $x$ -position position of point P in body 4. Figures 10 and 11 summarize the results obtained from the inverse kinematics stage.

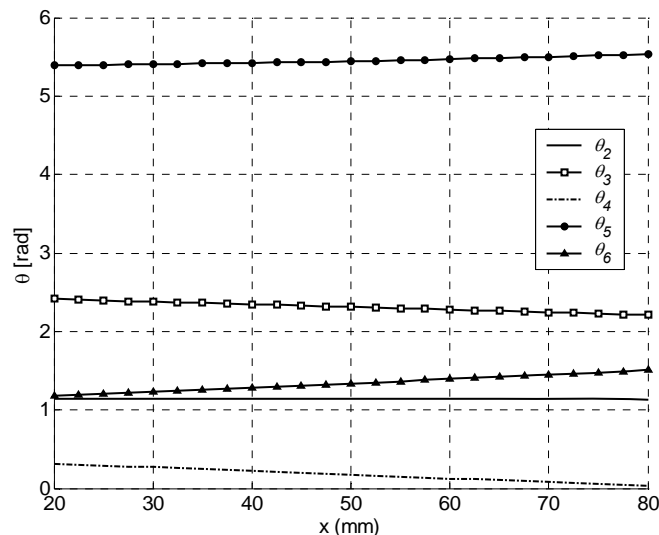
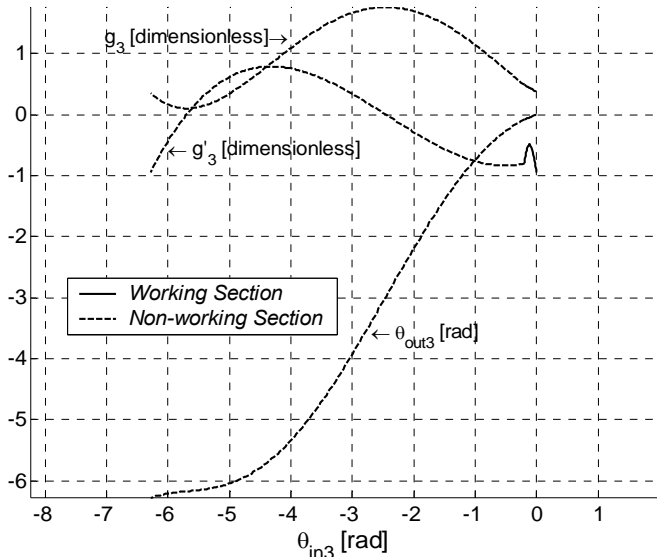


Fig. 11 Link angles versus point P  $x$ -position.  
Motion generation of  $f(x) = ax^2+bx+c$

The results corresponding to the profile synthesis are presented in Figs. 12 and 13. The output angles, I/O relationships, and derivative of the I/O relationships with respect to the input angle are shown for each connection, for working and non-working profiles. Figure 12 summarizes the

parameters corresponding to the connection 234. Similarly, Fig. 13 displays the results associated with the connection 456.



**Fig. 12 Output angle, I/O relationship and I/O derivative versus input angle, connection 234. Motion generation of  $f(x) = ax^2+bx+c$**

There is an apparent discontinuity for  $g'$  observed in Figs. 12 and 13 at  $\theta_{in}=\theta_{int}$  for the input angle. This discontinuity does not have any effect on the smoothness of the profile; however, it can be avoided by adding one more boundary condition to the non-working profile

$$g_w''(\theta_{int}) = g_{nw}''(\theta_{int})$$

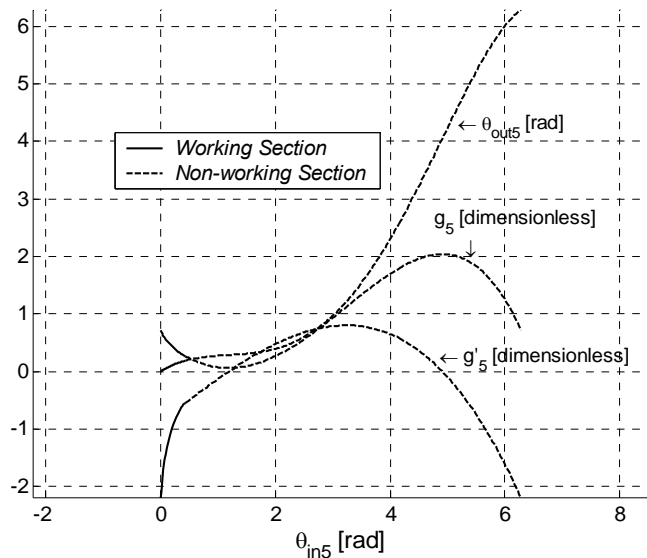


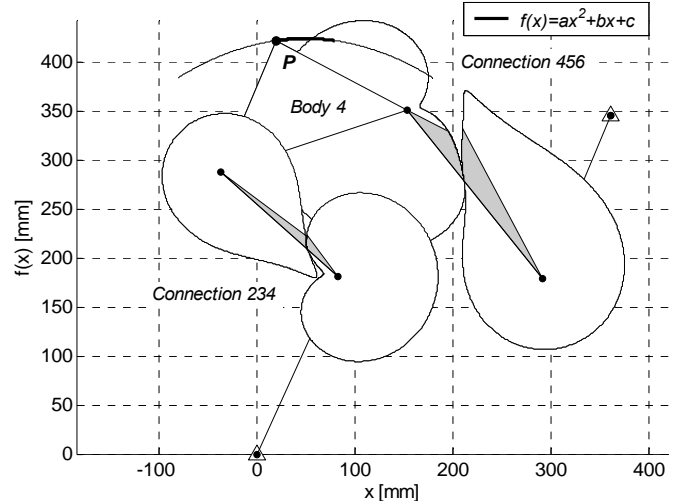
**Fig. 13 Output angle, I/O relationship and I/O derivative versus input angle, connection 456. Motion generation of  $f(x) = ax^2+bx+c$**

At this point, it is possible to plot the pitch curve because the I/O relationships were successfully extended through  $2\pi$  for the input angle. From Table 1, the center distances are  $l_3=160mm$  for the connection 234 and  $l_5=220mm$  for the connection 456.

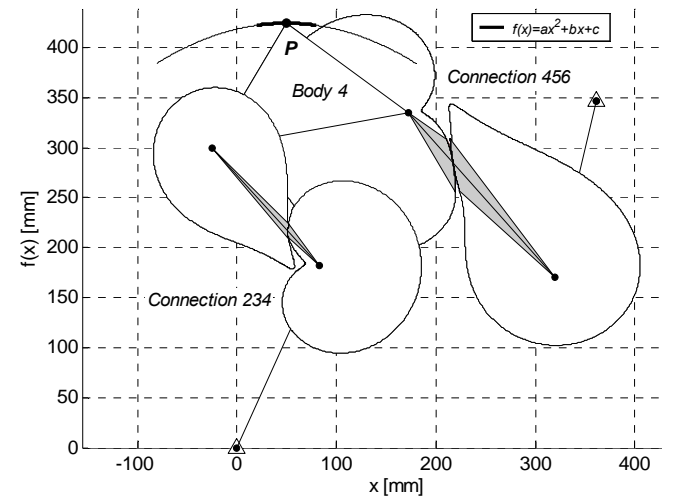
The final product of the design process is shown in Fig. 14, where the schematic six-link mechanism is presented at three different positions of the interval. The pitch profiles are also depicted. Working and non-working profiles are easily distinguished.

The overlap between the elements shown in Fig. 14 seems to be a difference with the hypothetical model early presented in Fig. 1. This is not a problem because each pair of gears occupies its own distinct plane of action.

One last observation is the number of positions that can theoretically be satisfied by this procedure, this is one of the advantages of this method. In this case ( $x_o=80mm$ ,  $x_f=20mm$ , and  $\Delta x=0.5mm$ ), a total of 121 positions that did not lie on a straight line were achieved with a 1-DOF mechanism.



**(a) Initial position  $x=20mm$**



**(b) Intermediate position  $x=50mm$**

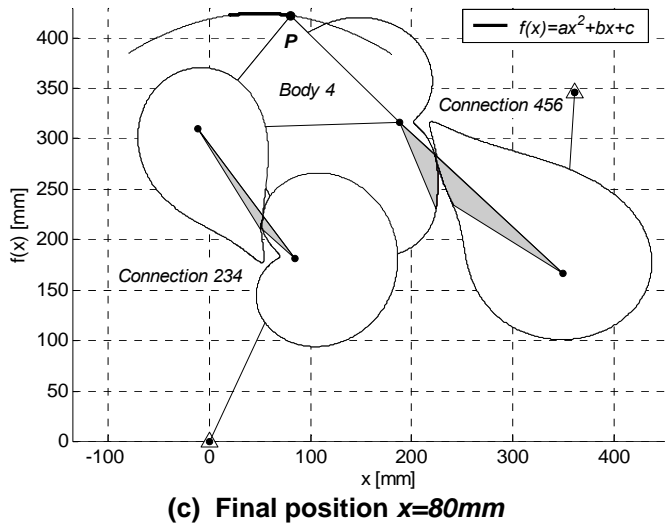


**Fig. 14 6-Link mechanism at three positions.  
Motion generation:  $f(x) = ax^2 + bx + c$**

## CONCLUSION

A two step procedure was introduced to perform motion generation using a 1-DOF planar mechanism that incorporates two non-circular gear pairs. First, the position problem is solved using an inverse kinematic analysis. Second, the profile of the gear pairs were determined that would satisfy the motion requirements.

An example was presented for the case of a point following a path that was defined by a quadratic function. The angle between the coupler link and the tangent to the path remained constant throughout the motion. The non-circular pitch profiles were theoretically synthesized for the motion requirements. In theory, the method enables one to satisfy a large amount of points. At the real application stage, manufacturing errors and physical space constraints can introduce more variables that will increase the structural error.

Three interesting future works derived from this report are presented. A variable orientation angle for the coupler will increase the nonlinearity of the system and introduce some modifications on the process. Development of a routine that includes the synthesis of the link lengths at first stage will contribute to the future implementation of the mechanism into real applications. The optimization of the mechanism in order to minimize the non-circularity of the gears without increasing the structural error will facilitate manufacturing of the mechanism.

## ACKNOWLEDGMENTS

The authors gratefully acknowledge the support provided by the Department of Energy via the University Research Program in Robotics (URPR), grant number DE-FG04-86NE37967.

The first author wants to acknowledge the support received from the Department of Mechanical Engineering-University of Puerto Rico at Mayagüez during the early phase of this work.

## REFERENCES

- [1] Holditch, H. On rolling curves. *Trans. Phys. Soc. (Lond.)*, 1842, (7), 61-82.
- [2] Cunningham F. W. Designing and using non-circular gears to generate mathematical functions. *Journal of Machine Design*. Feb. 19, 1959, pp. 161-164.
- [3] Freudenstein F. and Primrose E. J. F. Geared five-bar motion. *Trans. ASME, 85E (J. App. Mech. 30)*, 1963, 161-175.
- [4] Roth B. and Freudenstein F. Synthesis of path-generating mechanisms by numerical methods. *Trans. ASME (J. Engng. Ind. 30)*, 1963, 298-305.
- [5] Oleksa S. A. and Tesar D. Multiply separated position design of the geared five-bar function generator. *Trans. ASME (J. Engng. Ind.)*, 1963, 298-305.
- [6] Erdman A. G. and Sandor G. N. Kinematic synthesis of a geared five-bar function generator. *Trans. ASME, J. Engng. for Industry*, 1971, 11-16.
- [7] McLarnan C. W. Synthesis of six-link plane mechanism by numerical analysis. *Trans. ASME 85B (J. Engng. Ind. 30)*, 1963, 5-11.
- [8] Erdman A. G. and Sandor G. N. Kinematic synthesis of a geared five-bar function generator. *Journal of Engineering for Industry*, 1971, 93, B, No. 1, 157-164.
- [9] Dimarogonas A. D., Erdman G. N. and Sandor A. G. Synthesis of a geared  $N$ -bar linkage. *Trans. ASME (J. Engng. Ind.)*, 1971, 157-164.
- [10] Sandor, G. N., Rao A. V. and S. N. Kramer. Geared six-bar design. *Proceedings of the 2<sup>nd</sup> OSU Applied Mechanics Conference, Stillwater, Oklahoma, Oct. 7-9, 1971*. pp 25-1 to 25.13.
- [11] Dooner D. B. Function generation utilizing an eight-link mechanism and optimized non-circular gear elements with application to automotive steering. *Trans. ASME, J. Mech. Des.*, 2001, 215, 847-857.
- [12] Han J. Y. Complete balancing of the shaking moment in spatial linkages by adding planar noncircular gears. *Archive of Applied Mechs*, 1997, 67, 44-49.
- [13] Emura T. and Arakawa A. A new steering mechanism using noncircular gears. *Int. J. Jap. Soc. Mech. Engrs, Series III*, 1992, 35(4), 604-610.

- [14] Dooner, D. B. Use of noncircular gears to reduce torque and speed fluctuations in rotating shafts. *Trans. ASME, Journal of Mechanical Design*, 1997, 119, 299-306.
- [15] Yao, Y-A. and Yan H-S. A new method for torque balancing of planar linkages using non-circular gears. *Proc. Instn Mech. Engrs*, 2003, Vol. 217, Part C, 495-503.
- [16] Kochev, I. S. General method for active balancing of combined shaking moment and torque fluctuations in planar linkages. *Mech. Mach. Theory*, 1990, Vol. 25, No. 6, 679-687.
- [17] Figliolini, G. and Angeles, J. The synthesis of elliptical gears generated by shaper-cutters. *Trans. ASME, J. Mech. Des.*, 2003, 125, 793-801.
- [18] Litvin F. Gear geometry and applied theory. 1994. (Pearson Professional Education, USA).
- [19] Dooner D. B. and Seireg A. A. The kinematic geometry of gearing. New York: John Wiley & Sons Inc. 1995.
- [20] Dooner D. On the three laws of gearing. *Trans. ASME, J. Mech. Des.*, 2002, 124, 733-744.